CrossMark

Seasonal characteristics of oxalic acid and related SOA in the free troposphere of Mt. Hua, central China: Implications for sources and formation mechanisms

Jingjing Meng [a,b], Gehui Wang [a,c,*], Jianjun Li [a], Chunlei Cheng [a,b], Yanqin Ren [a,b], Yao Huang [a,b], Yuting Cheng [a,b], Junji Cao [a], Ting Zhang [a]

[a] State Key Laboratory of Loess and Quaternary Geology, Institute of Earth Environment, Chinese Academy of Sciences, Xi'an 710075, China
[b] University of Chinese Academy of Sciences, Beijing 100049, China
[c] School of Human Settlements and Civil Engineering, Xi'an Jiaotong University, Xi'an 710049, China

HIGHLIGHTS

- High abundances of oxalic acid and related SOA in the free troposphere of Mt. Hua, central China.
- Significant seasonal differences in sources and formation mechanisms of SOA.
- Increasing RH is unfavorable for oxalic acid formation.

ARTICLE INFO

ABSTRACT

PM_{10} aerosols from the summit of Mt. Hua (2060 m a.s.l) in central China during the winter and summer of 2009 were analyzed for dicarboxylic acids, ketocarboxylic acids and α-dicarbonyls. Molecular composition of dicarboxylic acids (C_2–C_{11}) in the free tropospheric aerosols reveals that oxalic acid (C_2, 399 $\pm$ 261 ng m^{-3} in winter and 522 $\pm$ 261 ng m^{-3} in summer) is the most abundant species in both seasons, followed by malonic (C_3) and succinic (C_4) acids, being consistent with that on ground levels. Most of the diacids are more abundant in summer than in winter, but adipic (C_6) and phthalic (Ph) acids are twice lower in summer, suggesting more significant impact of anthropogenic pollution on the wintertime alpine atmosphere. Moreover, glyoxal (Gly) and methylglyoxal (mGly) are also lower in summer (12 $\pm$ 6.1 ng m^{-3}) than in winter (22 $\pm$ 13 ng m^{-3}). As both dicarbonyls are a major precursor of C_2, their seasonal variation patterns, which are opposite to those of the diacids, indicate that the mountain troposphere is more oxidative in summer.

C_2 showed strong linear correlations with levoglucosan in winter and oxidation products of isoprene and monoterpene in summer. PCA analysis further suggested that the wintertime C_2 and related SOA in the Mt. Hua troposphere mostly originate from photochemical oxidations of anthropogenic pollutants emitted from biofuel and coal combustion in lowland regions. On contrast, the summertime C_2 and related SOA mostly originate from further oxidation of the mountainous isoprene and monoterpene oxidation products. The AIM model calculation results showed that oxalic acid concentration well correlated with particle acidity ($R^2 = 0.60$) but not correlated with particle liquid water content, indicating that particle acidity favors the organic acid formation because aqueous-phase C_2 production is the primary mechanism of C_2 formation in ambient aerosols and is driven by acid-catalyzed oxidation.

© 2014 Elsevier B.V. All rights reserved.

1. Introduction

Secondary organic aerosols (SOA) take an important role in climate change via affecting solar radiation. Dicarboxylic acids and related organic compounds are a typical class of SOA in the atmosphere (Mkoma and Kawamura, 2013) and omnipresent in precipitation (Sempéré and Kawamura, 1996), cloud water (Na et al., 2007) and fog (Kawamura et al., 1985). Because they are highly water-soluble (Sempéré and Kawamura, 1994), dicarboxylic acids can activate as cloud condensation nuclei (CCN) and thus influence cloud formation (Gierlus et al., 2012; Myriokefalitakis et al., 2011). They can be directly emitted from primary sources such as fossil fuel combustion, biomass burning and cooking (Fu et al., 2013; Mkoma and Kawamura, 2013; Wang et al., 2009, 2010, 2012a), but atmospheric dicarboxylic acids largely originate from

photochemical oxidation of organic precursors in either the gas phase or the liquid phase of aerosols (Kawamura et al., 2004; Myriokefalitakis et al., 2011). Oxalic acid (C_2) is often the predominant species of dicarboxylic acids in ambient particles, whose concentration in the atmosphere varies from ten nanograms per cubic meter in remote region (Kawamura et al., 1996a, b) to hundreds even more than one thousand nanograms per cubic meter in urban regions (Ho et al., 2007). Laboratory experiments have proposed the production of oxalic acid by an aqueous phase oxidation of precursors such as glyoxal (Gly), methylglyoxal (mGly) and pyruvic acid (Pyr) (Carlton et al., 2006; Ervens et al., 2011), which are formed by the gas-phase oxidation of reactive organic compounds (Lim et al., 2005) and are believed to irreversibly partition into the aerosol aqueous phase (Fu et al., 2008). In addition, oxalic acid can also be produced from high-molecular-weight compounds in aerosol-phase via multiple generations of oxidation (Cheng et al., 2013; Kroll and Seinfeld, 2008; Meng et al., 2013).

Investigation on dicarboxylic acids and related SOA has been conducted in various environments such as urban (Cheng et al., 2013; Ho et al., 2007; Kawamura and Yasui, 2005; Zhao et al., 2014), remote marine (Fu et al., 2013; Kawamura and Usukura, 1993), forest (Narukawa et al., 1999) and high-altitude background regions (Meng et al., 2013), most of which have been performed on the ground surface. Aircraft measurement found a pervasive layer of dicarboxylic acids above the clouds over the inland Huston area and the Gulf of Mexico, USA and the East Pacific Ocean (Sorooshian et al., 2007a, b), which suggests an important role of the organic acids such as CCN in the free troposphere that is the upper part of the troposphere and usually 1–2 km above the ground (Seinfeld and Pandis, 1998). High level of dicarboxylic acids on the ground surface has frequently been found in Chinese urban and rural areas (Cheng et al., 2013; Wang et al., 2006b, 2010), but very few information about dicarboxylic acids in the free troposphere over China has been documented (Kawamura et al., 2013a,b). Observation at alpine area is an alternative method for free tropospheric aerosol characterization, which is of advantages of long-term and low-cost compared to aircraft-and balloon-based measurements. Atmospheric environment of alpine regions is different from that in lowland regions due to stronger solar radiation and more significant variations in temperature and humidity, thus physical and chemical properties of alpine aerosols are different from those in lowland areas. Moreover, compared to the aerosols on the ground surface, impact on cloud formation by alpine aerosols may be more significant as they are more accessible to clouds due to high altitude. Mt. Hua is the highest mountain in central China and situated at the east border of Guanzhong Basin (Fig. 1), one of the most heavily polluted regions in the world (van Donkelaar et al, 2010). The west peak of Mt. Hua faces directly toward Guanzhong Basin. In 2009 we have collected 1-year term of aerosol samples including TSP, PM_{10} and size-segregated aerosols. Our previous studies focused on primary organic aerosols (Li et al., 2011, 2012), biogenic secondary organic aerosols (Li et al., 2013), and dust storm impact on the mountain aerosol chemistry (Wang et al., 2011, 2012b, 2013). In the current work we further focus on SOA particularly dicarboxylic acids, including oxalic acid, ketocarboxylic acids and dicarbonyls. We first investigate seasonal variations in abundances and compositions of oxalic acid and related SOA in the troposphere over Mt. Hua during winter and summer, and compare the results with those in lowland regions. Then we explore the impact of temperature (T), relative humidity (RH) and particle acidity (pH_{IS}) and liquid water content (LWC) on oxalic acid and related SOA to explore the sources and formation pathways of SOA in the free troposphere over central China.

2. Experiment

2.1. Ambient PM_{10} aerosol collection

PM_{10} samples were collected at the summit of Mt. Hua (2060 m a.s.l; 34°29′N, 110°05′E) during winter (January 10–22) and summer (July 15–August 25) of 2009 using a mid-volume air sampler (KC-120H, Qingdao Laoshan Company, China) equipped with prebaked (450 °C, 8 h) quartz fiber filters (Whatman, USA) at an airflow rate of 100 L min^{-1}. The winter sample was collected each for 12 h on a day/night basis in order to investigate the diurnal variation, while the summer sample was collected each for 24 h in order to obtain enough materials on the filter. A total of 21 samples (daytime: 10; nighttime: 11) were collected in the winter and 34 samples were collected in the summer. After sampling each sample was sealed in an aluminum foil bag and stored in a freezer at −20 °C prior to analysis. Field blank samples were also collected before and after the sampling by mounting a prebaked blank filter onto the sampler for about 10 min without sucking any air.

Fig. 1. A map description for the location of Mt. Hua.

2.2. Sample analyses

2.2.1. Dicarboxylic acids, ketocarboxylic acids and α-dicarbonyl analysis

Detailed methods for determining water-soluble dicarboxylic acids, ketocarboxylic acids and α-dicarbonyls in aerosols have been documented elsewhere (Kawamura et al., 1996a, Kawamura and Sakaguchi, 1999). Briefly, an aliquot of the PM_{10} samples was extracted with pure Milli-Q water, concentrated to nearly dry, and derivatized with 14% BF_3/n-butanol at 100 °C for 1 h. After the derivatization the derivatives were dissolved in n-hexane and washed with pure water three times. Finally, the hexane layer was concentrated and quantitatively analyzed using a capillary gas chromatography (GC; HP 6890) equipped with a split/splitless injector and a flame ionization detector. The oven temperature of GC was enhanced from 50 °C (2 min) to 120 °C at 15 °C min^{-1} and then to 300 °C at 5 °C min^{-1} with a final isothermal hold at 300 °C for 16 min. Peak identification was conducted by comparing the GC retention time with that of authentic standards and confirmed by mass spectrum of the sample using an Agilent 7890A gas chromatography coupled with a 5975C mass spectrometry (GC–MS).

Recovery experiment was conducted by spiking the free diacid standards onto a blank quartz fiber filter, then extracted and analyzed using the same method above. The recoveries were 85% for oxalic and higher than 90% for other target compounds. The amounts of target compounds in the field blanks were less than 4% of those in the ambient samples. Concentrations of all determined compounds reported here were corrected for both field blanks and recoveries.

2.2.2. Inorganic ions, elemental carbon (EC), organic carbon (OC) and organic aerosols

Inorganic ions, EC, OC and BSOA in the samples have been reported by Li et al (2012, 2013) and cited here to investigate the sources and formation mechanisms of oxalic acid and related SOA. Detailed analytical method of inorganic ions, EC and OC can be found in Li et al (2011, 2012), while the analytical details for organic aerosols can be found in Li et al (2012, 2013). Inorganic ions in the PM_{10} samples were measured by Dionex 600 ion chromatography (USA),while EC and OC in the samples were measured by DRI model 2001 carbon analyzer following the Interagency Monitoring of Protected Visual Environments (IMPROVE) thermal/optical reflectance (TOR) protocol. Organic aerosols in the samples were extracted using a mixture of methanol and dichloromethane, derivatized with N,O-bis-(trimethylsilyl) trifluoroacetamide (BSTFA) and measured using gas-chromatography/mass spectrometry (Agilent 5890/7593, USA).

2.2.3. Water-soluble organic (WSOC), water-soluble inorganic carbon (WSIC) and water-soluble organic nitrogen (WSON)

An aliquot of the PM_{10} sample was cut into pieces, extracted with Milli-Q water three times under sonication and filtered through PTFE filters to remove the filter debris and particles. The combined water-extracts were analyzed for water-soluble organic carbon (WSOC), water-soluble inorganic carbon (WSIC) and water-soluble total nitrogen (WSTN) using Shimadzu TOC-L CPH Total Carbon/Nitrogen Analyzer. Major water-soluble inorganic nitrogen (WSIN) species in atmospheric aerosols are NO_3^- and NH_4^+, thus the difference between WSTN and WSIN is defined as water-soluble organic nitrogen (WSON)(Wang et al., 2013).

3. Results and discussion

3.1. General description of chemical composition of PM_{10} in Mt. Hua

Concentrations of dicarboxylic acids, ketocarboxylic acids, α-dicarbonyls, WSOC, WSON, EC, OC and inorganic ions in the Mt. Hua PM_{10} samples are summarized and shown in Table 1. Concentrations of OC, EC and WSOC correlated well one another in winter ($R^2 > 0.53$, $p < 0.01$) and are around 1.5 times higher in winter than in summer.

Our previous study (Li et al., 2013) found that biomass burning tracers (i.e, levoglucosan, galactosan and manosan) and coal combustion tracers (i.e., polycyclic aromatic hydrocarbons (PAHs)) in the Mt. Hua samples are four times more abundant in winter than in summer, which is ascribed to an enhanced burning of biofuel and coal for house heating in the cold season. Relative abundances of water-soluble organic nitrogen (WSON) to water-soluble total nitrogen (WSTN) in the PM_{10} samples are 32% ± 8% in winter and 33% ± 7% in summer, respectively, which are similar to those detected in lowland regions like Xi'an city, China (Wang et al., 2013) and indicate that inorganic nitrogen compounds (i.e., nitrate and ammonium) are major water-soluble nitrogen-containing species in the mountain atmosphere. Our previous observation found that the summit (2060 m, a.s.l.) of Mt. Hua is above the planetary boundary layer in winter and aerosols in the wintertime troposphere are mostly derived from long-range transport (Li et al., 2012, 2013). Therefore, EC, OC, WSOC, dicarboxylic acids and related SOA exhibited similar concentrations between day and night in the cold season (see Table 1). In the current study we did not discuss the diurnal variations. Instead, in the following sections we averaged the winter concentrations and compared with the summer data to investigate the seasonality.

3.2. Seasonality of oxalic acid and related SOA

A series of dicarboxylic acids (C_2–C_{11}), ketocarboxylic acids (C_2–C_9) and α-dicarbonyls in the samples were detected (Table 1). Relative abundance of these compounds in winter and summer are shown in Fig. 2. As seen in Table 1, concentrations of total dicarboxylic acids in the Mt. Hua samples are 638 ± 377 ng m^{-3} (range: 132–1777 ng m^{-3}) in winter and 744 ± 340 ng m^{-3} (range: 50–1491 ng m^{-3}) in summer, which are 20%–30% lower than those in Asian lowland regions such as 14 Chinese cities (winter: 904 ± 480 ng m^{-3}; summer: 892 ± 457 ng m^{-3}) (Ho et al., 2007) but about 2–4 times higher than those in Asian elevated regions such as Nainital in central Himalayan (winter: 437 ng m^{-3}; summer: 430 ng m^{-3}) (Hegde and Kawamura, 2012) and Qinghai Lake in Tibetan Plateau (summer: 231 ± 119 ng m^{-3}) (Meng et al., 2013). The most abundant dicarboxylic acid is oxalic acid (C_2), accounting for 62% ± 6% and 69% ± 8% of the total in winter and summer, respectively, followed by malonic acid (C_3) (15% ± 4% versus 11% ± 3%) and succinic acid (C_4) (7% ± 2% versus 4% ± 1%). In summer the fourth most abundant species is azelaic acid (C_9) (23 ± 19 ng m^{-3}, Table 1), which is about twice higher than in winter (15 ± 11 ng m^{-3}, Table 1), suggesting enhancements in emission of biogenic unsaturated fatty acids (e.g., $C_{18:1}$) from terrestrial high plants and subsequent photo-oxidation in the warm season because C_9 is an oxidation product of biogenic unsaturated fatty acids containing a double bond at the C-9 position (Kawamura and Gagosian, 1987). On contrast, phthalic acid (Ph) is the fourth most abundant species in winter (see Fig. 2) and twice higher in winter than in summer (21 ± 14 ng m^{-3} versus 9.7 ± 5.7 ng m^{-3}, Table 1), further suggesting the enhanced emissions from coal burning in the cold season because Ph is produced from the oxidation of polycyclic aromatic hydrocarbons (PAHs) such as naphthalene that are mainly derived from Chinese domestic coal combustion (Kawamura and Ikushima, 1993; Li et al., 2012, Wang et al., 2006a, 2007).

Total ketocarboxylic acids in the Mt. Hua samples are 41 ± 29 ng m^{-3} in winter and 58 ± 24 ng m^{-3} in summer, respectively. The most abundant ketocarboxylic acid in both seasons is glyoxylic acid (ωC_2). Our previous study on stable carbon isotope compositions of oxalic acid and related SOA demonstrated that ωC_2 is an important precursor of oxalic acid (Wang et al., 2012a, 2012b), which is initially formed from an aqueous-phase oxidation of glyoxal with OH radical and other oxidants and further oxidized into oxalic acid (Sorooshian et al., 2007a; Wang et al., 2012a, 2012b).

Unlike those of dicarboxylic and ketocarboxylic acids seasonal variations of α-dicarbonyls exhibited an opposite pattern, which is higher

Table 1
Concentrations of dicarboxylic acids, ketocarboxylic acids, α-dicarbonyls, elemental carbon (EC), organic carbon (OC), water-soluble organic carbon (WSOC) and water-soluble organic nitrogen (WSON) in the PM_{10} samples collected at the summit of Mt. Hua during winter and summer 2009.

Compounds	Winter			Summer
	Day (n = 10)	Night (n = 11)	Total (n = 21)	Total (n = 34)
I. Dicarboxylic acids (ng m^{-3})				
Oxalic, C_2	400 ± 219 (184–859)	398 ± 305 (80–1236)	399 ± 261 (80–1236)	522 ± 261 (32–1066)
Malonic, C_3	82 ± 24 (56–124)	82 ± 27 (26–131)	82 ± 25 (26–131)	85 ± 44 (6.4–187)
Succinic, C_4	47 ± 33 (12–105)	49 ± 34 (5–127)	48 ± 32 (5–127)	29 ± 14 (2.7–53)
Glutaric, C_5	6.4 ± 6.2 (0.1–19)	6.8 ± 6.8 (0.2–23)	6.6 ± 6.4 (0.1–23)	9.0 ± 4.2 (1.0–17)
Adipic, C_6	4.6 ± 3.3 (0.8–9.3)	3.0 ± 2.6 (0.6–8.7)	3.8 ± 3.0 (0.6–9.3)	1.5 ± 0.8 (0.2–3.4)
Pimelic, C_7	5.9 ± 4.3 (0.4–14)	4.8 ± 4.2 (0.4–16)	5.4 ± 4.2 (0.4–16)	1.9 ± 1.4 (0–5.1)
Suberic, C_8	4.5 ± 4.0 (0.6–12)	2.1 ± 2.4 (0.3–8.1)	3.3 ± 3.4 (0.3–12)	3.3 ± 2.6 (0.1–13)
Azelaic, C_9	15 ± 11 (0.5–29)	15 ± 11 (0.9–40)	15 ± 11 (0.5–40)	23 ± 19 (1.5–81)
Sebacic, C_{10}	1.6 ± 1.6 (0–4.6)	1.6 ± 1.8 (0.2–6.0)	1.6 ± 1.7 (0–6.0)	3.0 ± 3.2 (0.2–19)
Undecanedioic, C_{11}	2.5 ± 2.6 (0.3–9.4)	1.6 ± 1.5 (0.3–5.6)	2.1 ± 2.1 (0.3–9.4)	8.3 ± 4.5 (0.6–19)
Methylmalonic, iC_4	4.3 ± 6.2 (0.3–19)	4.2 ± 5.3 (0.3–18)	4.2 ± 5.6 (0.3–19)	4.7 ± 4.6 (0–17)
Mehtylsuccinic, iC_5	4.6 ± 3.1 (1.4–10)	4.9 ± 3.4 (0.6–13)	4.7 ± 3.2 (0.6–13)	3.3 ± 1.6 (0.4–6.1)
Methylglutaric, iC_6	4.1 ± 2.3 (0.7–6.8)	3.9 ± 2.2 (1.0–8.4)	4.0 ± 2.2 (0.7–8.4)	2.4 ± 1.4 (0–6.6)
Maleic, M	6.4 ± 5.2 (0.9–17)	7.2 ± 4.5 (0.8–16)	6.8 ± 4.7 (0.8–17)	2.9 ± 2.0 (0.3–11)
Fumaric, F	13 ± 10 (1.6–33)	13 ± 10 (1.3–34)	13 ± 10 (1.3–34)	6.7 ± 4.3 (1.1–23)
Methylmaleic, mM	8.9 ± 5.3 (2.5–17)	9.8 ± 6.4 (2.7–25)	9.4 ± 5.8 (2.5–25)	4.2 ± 3.4 (0–16)
Phthalic, Ph	25 ± 15 (0.5–47)	17 ± 11 (1.3–40)	21 ± 14 (0.5–47)	9.7 ± 5.7 (0.7–29)
Isophthalic, iPh	0.5 ± 0.4 (0–1.3)	1.7 ± 4.3 (0–15)	1.1 ± 3.1 (0–15)	1.7 ± 2.0 (0–9.9)
Terephthalic, tPh	1.2 ± 0.9 (0–2.9)	2.5 ± 4.2 (0.1–15)	1.9 ± 3.1 (0–15)	1.3 ± 1.2 (0–6.5)
Ketomalonic, kC_3	3.0 ± 2.1 (0–6.5)	3.4 ± 2.1 (0.4–6.8)	3.2 ± 2.1 (0–6.8)	13 ± 7.1 (0.7–30)
Ketopimelic, kC_7	3.0 ± 2.4 (1.0–9.0)	2.6 ± 2.9 (0.5–11)	2.8 ± 2.6 (0.5–11)	8.2 ± 4.9 (0.4–22)
Subtotal	643 ± 339 (296–1301)	633 ± 425 (132–1777)	638 ± 377(132–1777) (132–1777)	744 ± 340 (50–1491)
II. Ketocarboxylic acids (ng m^{-3})				
Pyruvic, Pyr	4.9 ± 4.8 (0.5–13)	5.0 ± 5.7 (0.2–22)	4.9 ± 5.2 (0.2–22)	24 ± 10 (1.3–49)
Glyoxylic, ωC_2	23 ± 16 (2.9–50)	24 ± 20 (4.6–76)	24 ± 18 (2.9–76)	26 ± 13 (2.8–57)
3-Oxopropanoic, ωC_3	3.0 ± 2.3 (0–6.5)	3.4 ± 2.4 (0.3–8.9)	3.2 ± 2.3 (0–8.9)	2.7 ± 1.4 (0.2–6.0)
4-Oxobutanoic, ωC_4	7.3 ± 4.4 (1.3–14)	6.2 ± 3.9 (1.4–16)	6.7 ± 4.1 (1.3–16)	3.6 ± 1.6 (0.1–6.8)
9-Oxononanoic, ωC_9	2.5 ± 0.8 (1.5–4)	2.2 ± 1.1 (1.0–5.3)	2.3 ± 1.0 (1.0–5.3)	2.1 ± 2.4 (0–7.7)
Subtotal	41 ± 27 (6.2–82)	41 ± 32 (7.6–127)	41 ± 29 (6.2–127)	58 ± 24 (4.3–109)
III. α-Dicarbonyls (ng m^{-3})				
Glyoxal, Gly	8.6 ± 5.4 (0.2–15)	9.1 ± 6.1 (1.2–22)	8.8 ± 5.6 (0.2–22)	2.3 ± 0.9 (0.8–4.8)
Methylglyoxal, mGly	13 ± 8.5 (3.5–28)	13 ± 7.5 (3.1–26)	13 ± 7.8 (3.1–28)	10 ± 5.4 (0.6–23)
Subtotal	22 ± 13 (3.7–42)	22 ± 13 (4.3–49)	22 ± 13 (3.7–49)	12 ± 6.1 (1.4–26)
Total detected	705 ± 376(313–1409)	697 ± 468(144–1953)	701 ± 416(144–1953)	732 ± 329(56–1625)
IV. Inorganic ions (μg m^{-3})				
K^+	0.3 ± 0.2 (0–0.5)	0.3 ± 0.2 (0.1–0.7)	0.3 ± 0.2 (0–0.7)	0.3 ± 0.1 (0–0.6)
Na^+	0.3 ± 0.4 (0–1.0)	0.2 ± 0.2 (0–0.6)	0.2 ± 0.3 (0–1.0)	0.3 ± 0.1 (0.1–0.7)
NH_4^+	1.6 ± 1.0 (0.2–3.2)	1.5 ± 0.9 (0.3–3.3)	1.6 ± 0.9 (0.2–3.3)	4.3 ± 2.5 (0.7–12)
Mg^{2+}	0.1 ± 0 (0–0.2)	0.1 ± 0 (0.1–0.2)	0.1 ± 0 (0–0.2)	0.1 ± 0.1 (0–0.2)
Ca^{2+}	1.4 ± 0.7 (0.1–2.7)	1.6 ± 0.7 (0.5–2.8)	1.5 ± 0.7 (0.1–2.8)	0.4 ± 0.3 (0.1–1.1)
NO_3^-	2.6 ± 1.7 (0.5–5.5)	2.9 ± 1.6 (1.0–6.2)	2.7 ± 1.7 (0.5–6.2)	1.4 ± 1.4 (0–5.8)
SO_4^{2-}	7.3 ± 4.4 (1.6–16)	7.3 ± 4.4 (2.4–15)	7.3 ± 4.4 (1.6–16)	21 ± 12 (3.5–56)
V. Other species (μg m^{-3})				
EC	0.8 ± 0.4 (0–1.1)	0.9 ± 0.5 (0–1.7)	0.8 ± 0.5 (0–1.7)	0.6 ± 0.3 (0.2–1.2)
OC	6.0 ± 2.4 (2.5–9.0)	6.0 ± 2.8 (2.5–10)	6.0 ± 2.5 (2.5–10)	3.5 ± 1.3 (0.3–6.3)
WSOC	3.3 ± 1.2 (1.4–4.8)	3.5 ± 1.3 (1.6–5.0)	3.4 ± 1.2 (1.4–5.0)	2.2 ± 0.9 (0.1–3.8)
WSON	1.0 ± 0.6 (0.2–1.8)	0.7 ± 0.4 (0.2–1.7)	0.8 ± 0.5 (0.2–1.8)	1.9 ± 1.3 (0.2–6.4)
PM_{10}	51 ± 27 (11–114)	56 ± 27(12–116)	54 ± 27(11–116)	43 ± 18 (12–84)
WSOC/OC (%)	57 ± 7.0 (49–71)	59 ± 6.1 (47–66)	58 ± 6.5 (47–71)	61 ± 13 (26–86)
WSON/WSTN (%)	36 ± 6.5 (24–45)	29 ± 7.5 (13–40)	32 ± 7.9 (13–45)	33 ± 6.6(15–50)

in winter than in summer (22 ± 13 ng m^{-3} versus 12 ± 6 ng m^{-3}, Table 1). Since glyoxal (Gly) and methylglyoxal (mGly) are the major precursors of oxalic acid (Calton et al., 2006; Fu et al., 2008; Loeffler et al., 2006; Wang et al., 2012a, 2012b; Warneck, 2003), the opposite pattern suggests that the mountainous atmospheric environment is more oxidative in summer. Table 2 summarizes the major sources and concentrations of global production of gaseous Gly and mGly. As shown in Table 2, the global production ratio of Gly/mGly is about 1:1 for anthropogenic sources and about 1:5 for biogenic sources. Since reactive uptake coefficients of Gly and m Gly by particles are similar (Fu et al., 2008; Volkamer et al., 2007; Zhao et al., 2006), thus it is expected that the concentration ratio of particulate Gly/mGly is

equivalent when anthropogenic sources are predominant and is about 1:5 when natural sources are predominant. From Table 1 it can be seen that in the Mt. Hua samples Gly is comparable to mGly in winter but about 5 times less than mGly in summer, which again indicates that both carbonyls in Mt. Hua is mainly derived from anthropogenic sources in winter but mainly from biogenic sources in summer. More discussion will be given later. It has been proposed that concentration ratio of C_3/C_4 increases along with an increase in ambient temperatures when dicarboxylic acids are derived from local sources (Pavuluri et al., 2010). As seen in Fig. 3b, C_3/C_4 ratio of the samples linearly correlates with the ambient temperature in summer ($R^2 = 0.54$, $p < 0.01$), further indicating that dicarboxylic
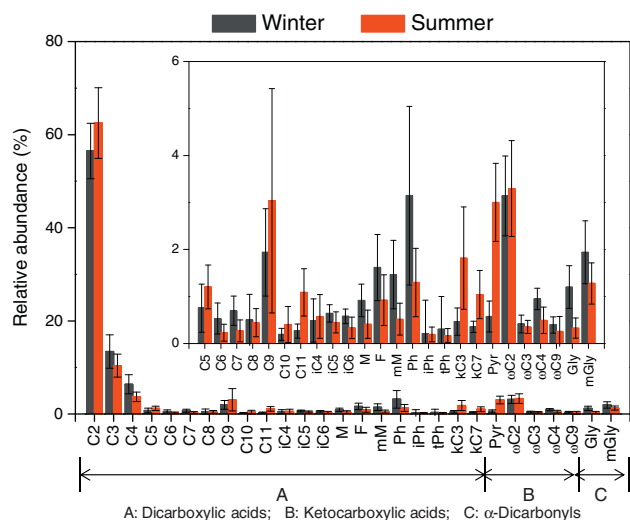
Fig. 2. Relative abundance of dicarboxylic acids, ketocarboxylic acids, and α-dicarbonyls in PM$_{10}$ collected in Mt. Hua during the winter and summer of 2009.

acids in the summertime samples are largely formed from local sources.

As seen in Fig. 4, concentration ratios of total dicarboxylic acids to WSOC, OC and PM$_{10}$ mass are 11.2% ± 3.3%, 6.5% ± 1.6% and 2.0% ± 0.7% in summer and two times higher than those in winter, indicating an enhanced photochemical production of SOA. The relative abundance of the total dicarboxylic acids to the particle mass (PM$_{10}$) is two times higher than that (1.1% ± 0.6% in summer, calculated from Meng et al. (2013)) in Qinghai Lake, Tibetan Plateau and three times higher than that (0.4% ± 0.1% in winter and 0.7% ± 0.3% in summer, calculated from Cheng et al.(2013)) in Xi'an, a megacity nearby Mt. Hua, further demonstrating an increased SOA production of the mountainous atmosphere in comparison with that on the ground surface. The summertime concentration of oxalic acid in Mt. Hua is, on average, about 10 times higher than that (0.03 ± 0.05 μg m^{-3} in 2005 and 0.03 ± 0.07 μg m^{-3} in 2006, respectively) (Sorooshian et al., 2007a) in the free troposphere over the Northeast Pacific Ocean, the Gulf of Mexico and the inland Huston areas, USA, suggesting a high level of organic particles in the free troposphere over inland China. The mass ratio (0.02 ± 0.02) of oxalic acid to sulfate in the Mt. Hua atmosphere is three times lower than that (0.06 ± 0.06) (Sorooshian et al., 2007a) in the North America region. Such a difference in free tropospheric aerosol composition between the two regions can be ascribed in part to high emission of SO$_2$ in inland China.

3.3. Linear fit regression and principal component analysis (PCA) for oxalic acid and related SOA

To further identify the sources and formation pathways of oxalic acid and related SOA in the Mt. Hua aerosols, we performed linear fit regression and principal component analysis (PCA) for the data

Table 2
Concentrations of α-dicarbonyls in the Mt. Hua samples and the global budgets of atmospheric glyoxal and methylglyoxal.

	Sources/season	Abundance	Mass ratio	
		Gly	mGly	Gly/mGly
Global budget	Biogenic	22.8[a]	113.5[a]	1:5
(Tg a^{-1})	Anthropogenic	22.2[a]	26.5[a]	1:1
Mt. Hua	Summer	2.3	10	1:4.4
(ng m^{-3},this study)	Winter	8.8	13	1:1.5

[a] Data are calculated from Fu et al., 2008.

sets of oxalic acid, sulfate and other tracers including levoglucosan, PAHs and n-alkanes which have been reported elsewhere (Li et al., 2011, 2012, 2013). We found that oxalic acid exhibited robust linear correlations with levoglucosan (R^2 = 0.61, p < 0.01, Fig. 5a) and sulfate in winter (R^2 = 0.83, p < 0.01, Fig. 5b) and with isoprene (R^2 = 0.75, p < 0.01, Fig. 5c) and α/β-pinene oxidation products (R^2 = 0.64, p < 0.01, Fig. 5d) in summer. Kawamura et al (2013a) reported a strong correlation between gaseous glyoxal and levoglucosan in the troposphere of Mt. Tai, east China and proposed that field burning wheat straw during the sampling period is the major sources. In this study a similar correlation was also found for glyoxal and levoglucosan (R^2 = 0.79, p < 0.01). After partitioning into aerosol aqueous phase, glyoxal further oxidizes into oxalic acid via a pathway similar to sulfate (Wang et al., 2012a, 2012b; Yu et al., 2005). Therefore, oxalic acid in the Mt. Hua wintertime samples well correlated with levoglucosan and sulfate (Fig. 5a and b). In contrast, the strong correlations between oxalic acid and the BSOA products suggest that biogenic volatile organic compounds (BVOCs) emitted from vegetation in the mountainous area are important precursors of oxalic acid and related SOA (Fig. 5c and d). Moreover, such correlations may indicate an important role of particle-phase reactions in SOA formation (Kroll and Seinfeld, 2008).

As seen in Table 3, PCA analysis extracted four components by the screen test, which account for 66%, 15%, 5% and 3% of the total variance in winter and 65%, 15%, 6% and 3% of the total variance in summer, respectively.

In winter, dicarboxylic acids (C$_2$–C$_7$ except C$_6$), ketocarboxylic aids, α-dicarbonyls, levoglucosan, SO$_4^{2-}$, NO$_3^-$, OC and WSOC showed high loadings (>0.50, Table 3) with the first component. Levoglucosan is a key marker of biomass burning, while SO$_4^{2-}$ and NO$_3^-$ are usually secondary photo-oxidation products. Thus, the first component can be categorized as photochemical oxidation of precursors emitted from biofuel combustion in lowland regions. Low-molecular-weight (LMW) n-alkanes and PAHs in China are mainly derived from domestic coal combustion (Wang et al., 2006a, 2007), thus the strong correlations of fossil fuel n-alkanes and PAHs with component 2 indicate the emissions from the household coal burning as an important source of oxalic acid and related SOA. Glyoxal and t-Ph presented high loading with component 3, suggesting an important contribution from the emissions of municipal wastes burning because t-Ph is mainly produced from the combustion of municipal solid wastes and plastic polymers (Simoneit et al., 2005). Moreover, glyoxal can also be produced from photochemical oxidation of p-xylene, which is a major raw material for plasticizer synthesis (Volkamer et al., 2001). Plant wax is the dominant source of high-molecular-weight (HMW) n-alkanes (Li et al., 2012), thus the associations of azelaic acid (C$_9$) and plant wax n-alkanes with the fourth component suggest a possible contribution from plant emission to total dicarboxylic acids, although it is not significant.

In summer dicarboxylic acids (C$_2$–C$_6$, and C$_9$), ketocarboxylic aids, α-dicarbonyls, three kinds of biogenic SOA (BSOA) tracers (oxidation products of isoprene, α-/β-pinene and β-caryophyllene), plant wax n-alkanes and WSOC exhibited strong correlations with the first component (Table 3). While C$_2$, C$_7$, β-caryophyllene products, plant wax n-alkanes and NO$_3^-$ well correlated with the second component. Thus both components represent the significant contribution of plant emissions and subsequent photochemical oxidation and account for 81% of the total variance, further demonstrating the predominance of biogenic sources of oxalic acid and related SOA in the summertime atmosphere of Mt. Hua. As shown in Table 3, the third and forth components associate with t-Ph, levoglucosan, F$^-$ and SO$_4^{2-}$, which are mainly derived from combustions of coal, biomass and solid wastes. The two components account for only 11% of the total variances, indicating an insignificant impact of human activity on the mountain SOA production during summer.
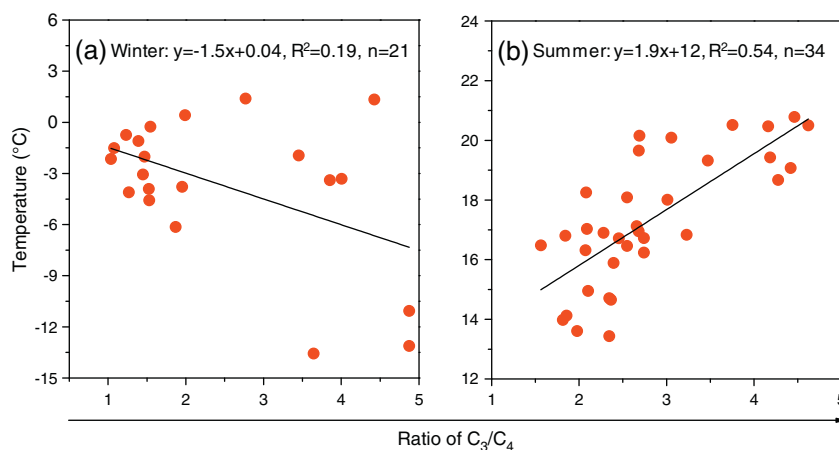
Fig. 3. Linear regression for temperature (T) with mass ratio of C_3/C_4 in (a) winter and (b) summer (see the abbreviations in Table 1).

3.4. Effects of temperature and relative humidity on the concentrations of oxalic acid and related SOA in summer

As discussed above, the wintertime SOA mainly derived from long-range transport rather than local photo-oxidation of biogenic precursors. Therefore, we only discussed the effect of meteorological factors on the formations of oxalic acid and related SOA in the summer samples. Temporal variations in concentrations of oxalic acid and related SOA and meteorological parameters during summer were plotted in Fig. 6. The concentrations of oxalic acid and related SOA reduced about 30–70% when it was rainy, which can be explained by a scavenging effect of wet deposition and/or a reduced SOA production due to decreases in solar radiation and biogenic emission. Here we selected three major SOA (i.e., oxalic acid, glyoxal and methylglyoxal) in the samples to discuss the impact of temperature and RH on their abundances.

Glyoxal ($R^2 = 0.18$) and methylglyoxal ($R^2 = 0.21$) in the Mt. Hua samples showed very weak correlations with the ambient temperatures.

Li et al (2013) have found that all the detected BSOA tracers including 2-methyltetrols and *cis*-pinonic acid in the Mt. Hua samples showed a strong positive correlation with temperatures because of enhancements in isoprene emission and BSOA production under higher-temperature conditions. However, lower-temperature is favorable for the partitioning of gas-phase products such as glyoxal and methylglyoxal to the aerosol liquid phase, which is governed by Henry's law (Myriokefalitakis et al., 2011). Oxalic acid exhibited a robust linear correlation with temperatures (Fig. 7a), largely due to enhanced photochemical oxidation under higher-temperature conditions.

Chamber studies (Gao et al., 2004; Jang et al., 2002) and field observations (Pathak et al., 2011) have demonstrated that acid-catalyzed heterogeneous reaction can enhance SOA production. Liquid water content (LWC) and acidity of a particle can influence significantly the formation of SOA via gas-to-particle partitioning of organic precursors and subsequent heterogeneous reactions on aerosol aqueous phase (Pathak et al., 2003). Particle acidity, which is often denoted as in-situ
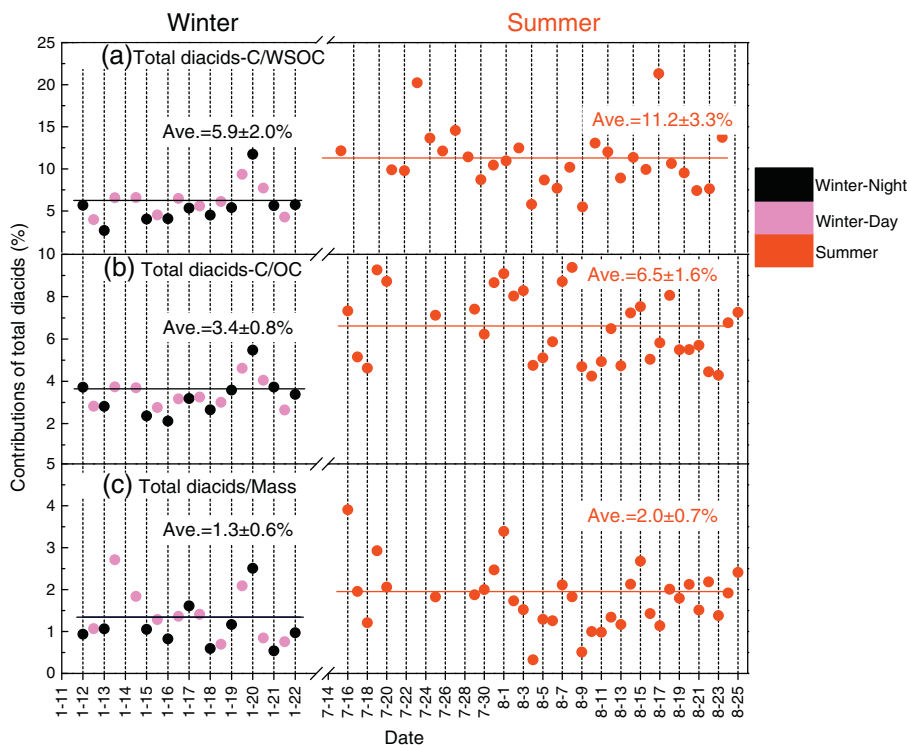

Fig. 4. Temporal variations in the contributions (%) of total diacids to (a) water-soluble organic carbon (WSOC), (b) organic carbon (OC), and (c) particle mass of PM_{10} (Mass) at the summit of Mt. Hua during winter and summer.
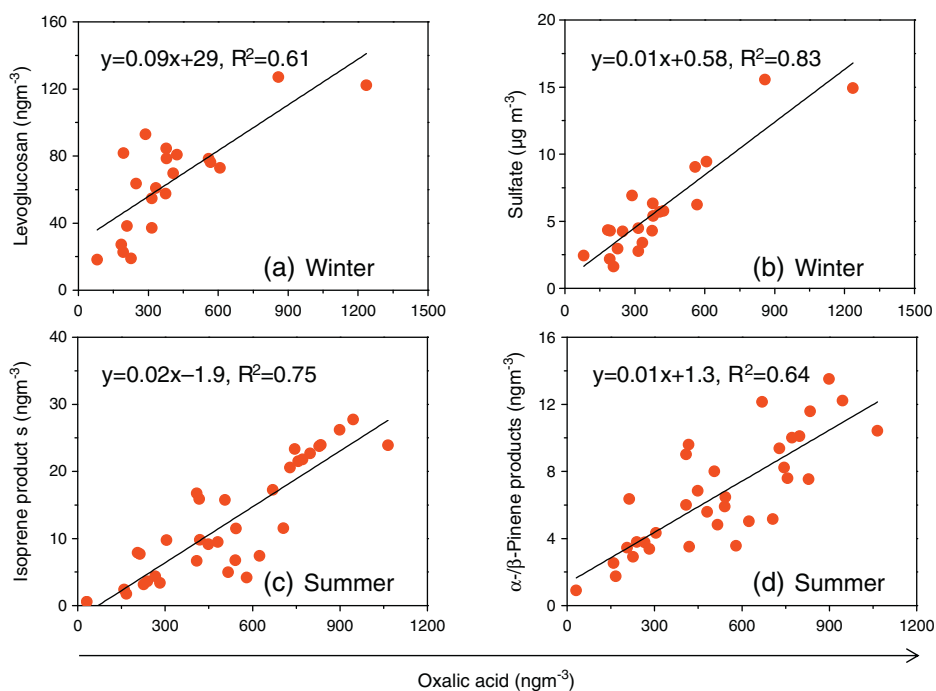
Fig. 5. Linear fit regressions for oxalic acid with levoglucosan, sulfate and isoprene and α-/β-pinene oxidation products (isoprene oxidation products: the sum of 2-methylglyceric acid + C_5-alkenetriols + 2-methyltetrols + 3-methyltetrahydrofuran-3,4-diols; α-/β-pinene oxidation products: the sum of *cis*-pinonic acid + 3-hydroxyglutaric acid + 3-methyl-1,2,3-butanetricarboxylic acid).

pH (pH_{IS}), and LWC cannot be directly measured and usually calculated using some models. LWC and pH_{IS} of the Mt. Hua samples have been calculated by Li et al (2013) using the Aerosol Inorganic Model (AIM) (Clegg and Brimblecombe, 1998a, b) and are cited here to explore the

effect of these two factors on the formation of oxalic acid and related SOA. As shown in Fig. 7b and c, no significant correlation was found for oxalic acid and LWC, but a robust negative correlation was obtained for oxalic acid and pH_{IS} ($R^2 = 0.60$), suggesting that acidic condition is

Table 3
Principal component analysis for major species detected in the PM_{10} samples from Mt. Hua in the winter and summer of 2009.

Winter (n = 21)					Summer (n = 34)				
Compounds	Factor 1	Factor 2	Factor 3	Factor 4	Compounds	Factor 1	Factor 2	Factor 3	Factor 4
C_2	**0.75**[a]	**0.52**	0.04	−0.03	C_2	**0.94**	**0.65**	−0.15	0.02
C_3	**0.71**	**0.54**	0.09	0.01	C_3	**0.88**	0.23	0.21	0.01
C_4	**0.89**	0.41	0.12	0.02	C_4	**0.80**	0.08	0.13	0.22
C_5	**0.94**	0.29	0.05	−0.04	C_5	**0.56**	0.21	0.38	0.03
C_6	0.11	**0.80**	−0.04	−0.13	C_6	**0.55**	0.14	0.26	0.31
C_7	**0.89**	0.28	0.20	0.13	C_7	0.08	**0.92**	0.02	0.15
C_9	0.32	**0.55**	0.06	−0.04	C_9	**0.82**	0.12	−0.05	0.06
M	0.42	**0.88**	0.04	−0.04	M	0.15	0.16	**0.72**	0.06
F	0.27	**0.93**	0.04	−0.06	F	0.02	0.11	**0.52**	**0.72**
Ph	0.28	**0.62**	−0.03	−0.08	Ph	0.38	0.02	**0.68**	0.07
t-Ph	0.06	0.08	**0.98**	0.05	t-Ph	0.03	0.08	**0.70**	0.22
ωC_2	**0.90**	0.39	0.02	0.13	ωC_2	**0.84**	0.24	0.12	0.12
Pyr	**0.79**	0.41	−0.07	0.40	Pyr	**0.73**	0.11	0.14	0.22
Gly	**0.53**	0.24	**0.57**	0.07	Gly	**0.89**	−0.08	−0.05	0.18
mGly	**0.82**	0.43	0.06	0.33	mGly	**0.84**	0.22	−0.12	−0.03
Plant wax *n*-alkanes[b]	0.04	0.12	0.08	**0.97**	Isoprene products[c]	**0.92**	0.23	0.01	−0.17
Fossil fuel *n*-alkanes[b]	0.23	**0.79**	0.08	0.01	α-/β-Pinene products[c]	**0.61**	**0.52**	−0.13	−0.06
PAHs[b]	0.02	**0.91**	0.12	−0.16	β-Caryophyllene product[c]	**0.62**	−0.05	0.23	0.11
Levoglucosan[b]	**0.91**	0.41	0.16	0.19	Plant wax *n*-alkanes[b]	**0.62**	**0.63**	0.01	−0.15
SO_4^{2-}	**0.90**	0.23	0.09	0.09	Fossil fuel *n*-alkanes[b]	0.13	0.06	0.92	0.03
NO_3^-	**0.57**	**0.76**	0.15	0.10	Levoglucosan[b]	0.05	0.22	0.04	**0.76**
OC	**0.56**	**0.55**	0.13	−0.15	SO_4^{2-}	0.33	0.42	0.22	**0.62**
EC	0.30	**0.79**	−0.08	0.01	NO_3^-	0.42	**0.65**	0.08	0.01
WSOC	**0.63**	**0.57**	0.30	0.17	OC				
					WSOC	**0.81**	0.15	0.11	0.21
Variance	66%	15%	5%	3%	Variance	65%	15%	6%	5%
Source	Biomass burning	Coal combustion	Solid waste	Biogenic	Source	Biogenic	Biogenic	Fossil fuel	Biomass burning

[a] Absolute values higher than 0.5 are highlighted in bold.
[b] Data are cited from Li et al., 2012.
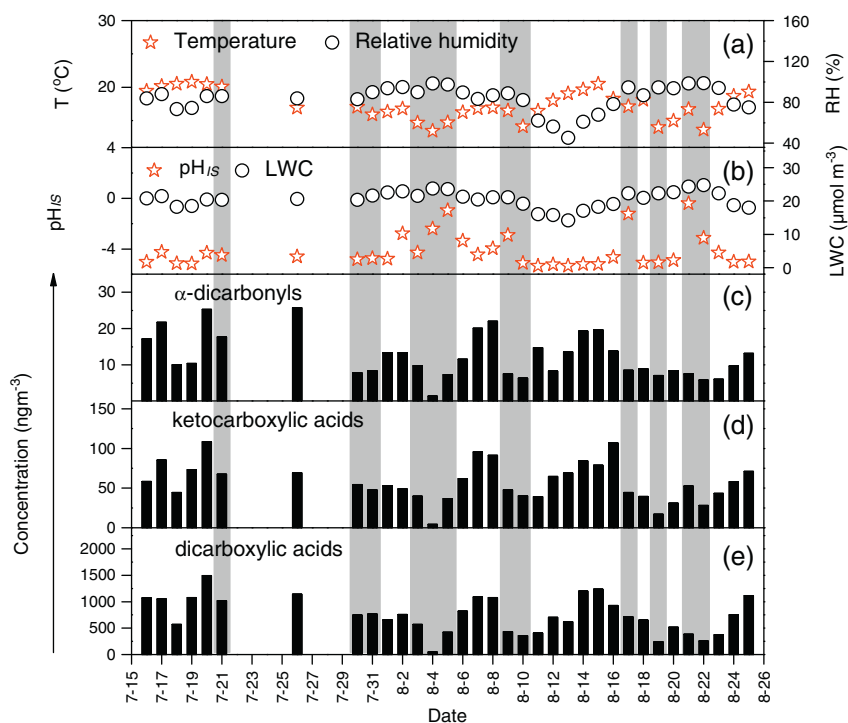[c] Data are cited from Li et al., 2013.

Fig. 6. Temporal variations of temperature, relative humidity, in-situ acidity of particles (pH$_{IS}$), liquid water content of particles (LWC), and concentrations of α-dicarbonyls, ketocarboxylic acids and dicarboxylic acids (rainy days are highlighted in shadow).

favorable for the organic acid formation. A multiple variable linear regression analysis showed that particle acidity (pH$_{IS}$) of the Mt. Hua aerosol is strongly dependent on RH and ammonium-to-sulfate molar ratio ([NH$_4^+$]/[SO$_4^{2-}$],$R_{N/S}$):

$$pH_{IS} = 4.9RH + 0.05R_{N/S} - 4.2$$

The equation indicates that high RH of the ambient air can reduce particle acidity (pH$_{IS}$) and is thus unfavorable for oxalic acid formation by acid-catalyzed reaction occurring in the aerosol aqueous phase. RH also controls the liquid water content (LWC) of aerosol (Volkamer et al., 2009). Lim et al (2005) observed an increase in organic acid concentrations along with an increase of LWC at the range of 0.25–1.0 g m^{-3}. However, a similar correlation was not observed for the Mt. Hua samples (Fig. 7b). Higher LWC can enhance the partitioning of the gaseous precursors into the aerosol aqueous phase but also can inhibit acid-catalyzed formation of oxalic acid and related SOA due to a decrease in aerosol acidity.

4. Summary and conclusion

Dicarboxylic acids (C$_2$–C$_{11}$), ketocarboxylic acids, α-dicarbonyls, EC, OC, WSOC and WSON in the PM$_{10}$ samples collected at the summit of Mt. Hua, central China during the winter and summer of 2009 were determined. Molecular compositions of dicarboxylic acids in the mountain free troposphere are similar to those on the ground surface in both seasons. Concentrations of dicarboxylic acids in the mountain atmosphere is 20%–30% lower than those on Chinese urban ground surface but 2–4 times higher than those in Asian elevated regions such as Himalaya region and Tibetan Plateau, indicating a high loading of organic particles in the atmosphere of inland China. Concentration ratios of total dicarboxylic acids to WSOC, OC and PM$_{10}$ mass are twice higher in summer than those in winter, indicating an enhanced photochemical production of SOA.

Source identification results showed that oxalic acid and related SOA in the wintertime atmosphere of Mt. Hua are mostly derived from photooxidation of anthropogenic pollutants that are transported from lowland regions via a long-distance. On contrast, oxalic acid and related SOA in the alpine atmosphere during summer are largely derived
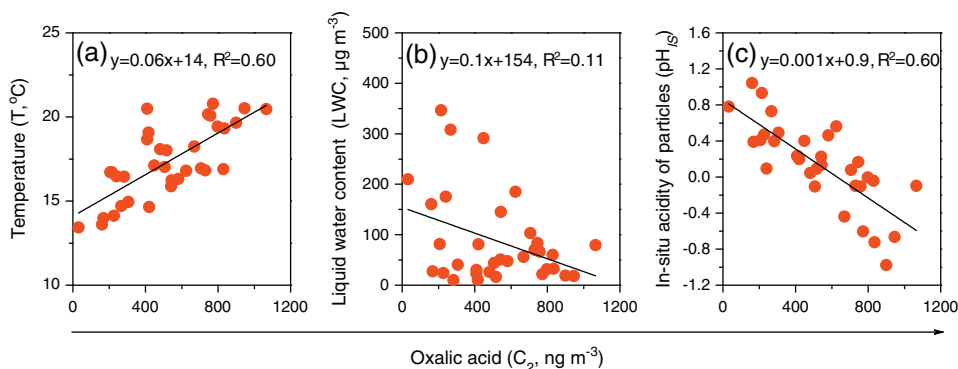

Fig. 7. Relationships between oxalic acid concentration and (a) temperature (T), (b) liquid water content (LWC), (c) in-situ acidity of particles (pH$_{IS}$).

from further photochemical oxidation of local isoprene and monoterpene oxidation products. Since higher temperature is unfavorable for the partitioning of gas-phase glyoxal and methylglyoxal to the aqueous phase but favorable for BVOCs emissions from mountain plants in summer, glyoxal and methylglyoxal in the samples exhibited very weak correlations with the ambient temperatures. On contrast, oxalic acid presented a strong correlation with the ambient temperatures. Based on the AIM model calculation, we found that increase in particle acidity (pH_{IS}) can result in enhancements in productions of oxalic acid and related SOA. An increase in relative humidity of the ambient air can reduce particle acidity (pH_{IS}) and thus suppress oxalic acid formation from isoprene and monoterpene oxidation products via acid-catalyzed reaction.

Conflict of interest

The authors declare that there are no conflicts of interest.

Acknowledgments

References

Carlton AG, Turpin BJ, Lim H-J, Altieri KE, Seitzinger S. Link between isoprene and secondary organic aerosol (SOA): pyruvic acid oxidation yields low volatility organic acids in clouds. Geophys Res Lett 2006;33. L06822.

Cheng C, Wang G, Zhou B, Meng J, Li J, Cao J, et al. Comparison of dicarboxylic acids and related compounds in aerosol samples collected in Xi'an, China during haze and clean periods. Atmos Environ 2013;81:443–9.

Clegg SL, Brimblecombe P. Thermodynamic model of the system $H^+-NH4^+-Na^+-SO_4^2-NO_3-Cl-H_2O$ at 298.15 K. J Phys Chem A 1998a;102:2155–71.

Clegg SL, Brimblecombe P. Thermodynamic model of the system $H^+-NH_4^+-SO_4^{2-}-NO_3^--H_2O$ at tropospheric temperatures. J Phys Chem A 1998b;102:2137–54.

Ervens B, Turpin BJ, Weber RJ. Secondary organic aerosol formation in cloud droplets and aqueous particles (aqSOA): a review of laboratory, field and model studies. Atmos Chem Phys 2011;11:11069–102.

Fu T-M, Jacob DJ, Wittrock F, Burrows JP, Vrekoussis M, Henze DK. Global budgets of atmospheric glyoxal and methylglyoxal, and implications for formation of secondary organic aerosols. J Geophys Res 2008;113. D15303.

Fu P, Kawamura K, Usukura K, Miura K. Dicarboxylic acids, ketocarboxylic acids and glyoxal in the marine aerosols collected during a round-the-world cruise. Mar Chem 2013;148:22–32.

Gao S, Ng NL, Keywood M, Varutbangkul V, Bahreini R, Nenes A, et al. Particle phase acidity and oligomer formation in secondary organic aerosol. Environ Sci Tech 2004;38:6582–9.

Gierlus KM, Laskina O, Abernathy TL, Grassian VH. Laboratory study of the effect of oxalic acid on the cloud condensation nuclei activity of mineral dust aerosol. Atmos Environ 2012;46:125–30.

Hegde P, Kawamura K. Seasonal variations of water-soluble organic carbon, dicarboxylic acids, ketocarboxylic acids, and α-dicarbonyls in Central Himalayan aerosols. Atmos Chem Phys 2012;12:6645–65.

Ho KF, Cao J, Lee SC, Kawamura K, Zhang R, Chow JC, et al. Dicarboxylic acids, ketocarboxylic acids, and dicarbonyls in the urban atmosphere of China. J Geophys Res 2007;112:D22S27.

Jang M, Czoschke NM, Lee S, Kamens RM. Heterogeneous atmospheric aerosol production by acid-catalyzed particle-phase reactions. Science 2002;298:814–7.

Kawamura K, Gagosian RB. Implications of ω-oxocarboxylic acids in the remote marine atmosphere for photo-oxidation of unsaturated fatty acids. Nature 1987;325:330–2.

Kawamura K, Ikushima K. Seasonal changes in the distribution of dicarboxylic acids in the urban atmosphere. Environ Sci Tech 1993;27:2227–35.

Kawamura K, Sakaguchi F. Molecular distributions of water soluble dicarboxylic acids in marine aerosols over the Pacific Ocean including tropics. J Geophys Res 1999;104:3501–9.

Kawamura K, Usukura K. Distributions of low molecular weight dicarboxylic acids in the North Pacific aerosol samples. J Oceanogr 1993;49:271–83.

Kawamura K, Yasui O. Diurnal changes in the distribution of dicarboxylic acids, ketocarboxylic acids and dicarbonyls in the urban Tokyo atmosphere. Atmos Environ 2005;39:1945–60.

Kawamura K, Steinberg S, Kaplan I. Capillary GC determination of short-chain dicarboxylic acids in rain, fog, and mist. Int J Environ Anal Chem 1985;19:175–88.

Kawamura K, Kasukabe H, Barrie LA. Source and reaction pathways of dicarboxylic acids, ketoacids and dicarbonyls in arctic aerosols: one year of observations. Atmos Environ 1996a;30:1709–22.

Kawamura K, Seméré R, Imai Y, Fujii Y, Hayashi M. Water soluble dicarboxylic acids and related compounds in Antarctic aerosols. J Geophys Res 1996b;101:18721–8.

Kawamura K, Kobayashi M, Tsubonuma N, Mochida M, Watanabe T, Lee M. Organic and inorganic compositions of marine aerosols from East Asia: seasonal variations of water-soluble dicarboxylic acids, major ions, total carbon and nitrogen, and stable C and N isotopic composition. In: Ronald J, Hill J, Kenneth P, editors. The Geochemical Society Special Publications, 9. Elsevier; 2004. p. 243–65.

Kawamura K, Okuzawa K, Aggarwal SH, Irie H, Kanaya Y, Wang Z. Determination of gaseous and particulate carbonyls (glycolaldehyde, hydroxyacetone, glyoxal, methylglyoxal, nonanal and decanal) in the atmosphere at Mt. Tai. Atmos Chem Phys 2013a;13:5369–80.

Kawamura K, Tachibana E, Okuzawa K, Aggarwal SH, Kanaya Y, Wang Z. High abundances of water-soluble dicarboxylic acids, ketocarboxylic acids and α-dicarbonyls in the mountaintop aerosols over the North China Plain during wheat burning season. Atmos Chem Phys 2013b;13:8285–302.

Kroll JH, Seinfeld JH. Chemistry of secondary organic aerosol: formation and evolution of low-volatility organics in the atmosphere. Atmos Environ 2008;42:3593–624.

Li J, Wang G, Zhou B, Cheng C, Cao J, Shen Z, et al. Chemical composition and size distribution of wintertime aerosols in the atmosphere of Mt. Hua in central China. Atmos Environ 2011;45:1251–8.

Li J, Wang G, Zhou B, Cheng C, Cao J, Shen Z, et al. Airborne particulate organics at the summit (2060 m, a.s.l.) of Mt. Hua in central China during winter: implications for biofuel and coal combustion. Atmos Res 2012;106:108–19.

Li J, Wang G, Cao J, Wang X, Zhang R. Observation of biogenic secondary organic aerosols in the atmosphere of a mountain site in central China: temperature and relative humidity effects. Atmos Chem Phys 2013;13:11535–49.

Lim H-J, Carlton AG, Turpin BJ. Isoprene forms secondary organic aerosol through cloud processing: model simulations. Environ Sci Tech 2005;39:4441–6.

Loeffler KW, Koehler CA, Paul NM, De Haan DO. Oligomer formation in evaporating aqueous glyoxal and methyl glyoxal solutions. Environ Sci Tech 2006;40:6318–23.

Meng J, Wang G, Li J, Cheng C, Cao J. Atmospheric oxalic acid and related secondary organic aerosols in Qinghai Lake, a continental background site in Tibet Plateau. Atmos Environ 2013;79:582–9.

Mkoma SL, Kawamura K. Molecular composition of dicarboxylic acids, ketocarboxylic acids, α-dicarbonyls and fatty acids in atmospheric aerosols from Tanzania, East Africa during wet and dry seasons. Atmos Chem Phys 2013;13:2235–51.

Myriokefalitakis S, Tsigaridis K, Mihalopoulos N, Sciare J, Nenes A, Kawamura K, et al. In-cloud oxalate formation in the global troposphere: a 3-D modeling study. Atmos Chem Phys 2011;11:5761–82.

Na K, Song C, Switzer C, Cocker DR. Effect of ammonia on secondary organic aerosol formation from α-pinene ozonolysis in dry and humid conditions. Environ Sci Tech 2007;41:6096–102.

Narukawa M, Kawamura K, Takeuchi N, Nakajima T. Distribution of dicarboxylic acids and carbon isotopic compositions in aerosols from 1997 Indonesian forest fires. Geophys Res Lett 1999;26:3101–4.

Pathak RK, Yao X, Lau AKH, Chan CK. Acidity and concentrations of ionic species of $PM_{2.5}$ in Hong Kong. Atmos Environ 2003;37:1113–24.

Pathak RK, Wang T, Ho KF, Lee SC. Characteristics of summertime $PM_{2.5}$ organic and elemental carbon in four major Chinese cities: implications of high acidity for water-soluble organic carbon (WSOC). Atmos Environ 2011;45:318–25.

Pavuluri CM, Kawamura K, Swaminathan T. Water-soluble organic carbon, dicarboxylic acids, ketoacids, and α-dicarbonyls in the tropical Indian aerosols. J Geophys Res 2010;115. D11302.

Seinfeld JH, Pandis SN. Atmospheric Chemistry and Physics: From air pollution to climate change. New York: John Wiley & Sons; 1998.

Sempéré R, Kawamura K. Comparative distributions of dicarboxylic acids and related polar compounds in snow, rain and aerosols from urban atmosphere. Atmos Environ 1994;28:449–59.

Sempéré R, Kawamura K. Low molecular weight dicarboxylic acids and related polar compounds in the remote marine rain samples collected from Western Pacific. Atmos Environ 1996;30:1609–19.

Simoneit BRT, Medeiros PM, Didyk BM. Combustion products of plastics as indicators for refuse burning in the atmosphere. Environ Sci Tech 2005;39:6961–70.

Sorooshian A, Lu M-L, Brechtel FJ, Jonsson H, Feingold G, Flagan RC, et al. On the source of organic acid aerosol layers above clouds. Environ Sci Tech 2007a;41:4647–54.

Sorooshian A, Ng NL, Chan AWH, Feingold G, Flagan RC, Seinfeld JH. Particulate organic acids and overall water-soluble aerosol composition measurements from the 2006 Gulf of Mexico Atmospheric Composition and Climate Study (GoMACCS). J Geophys Res 2007b;112. D13201.

van Donkelaar A, Martin RV, Brauer M, Kahn R, Levy R, Verduzco C, et al. Global estimates of ambient fine particulate matter concentrations from satellite-based aerosol optical depth: development and application. Environmental Health Perspectives 2010;118:8347–55.

Volkamer R, Platt U, Wirtz K. Primary and secondary glyoxal formation from aromatics: experimental evidence for the bicycloalkyl–radical pathway from benzene, toluene, and p-xylene. J Phys Chem 2001;105:7865–74.

Volkamer R, San Martini F, Molina LT, Salcedo D, Jimenez JL, Molina MJ. A missing sink for gas-phase glyoxal in Mexico City: formation of secondary organic aerosol. Geophys Res Lett 2007;34:L19807. http://dx.doi.org/10.1029/2007GL030752.

Volkamer R, Ziemann PJ, Molina MJ. Secondary organic aerosol formation from acetylene (C_2H_2): seed effect on SOA yields due to organic photochemistry in the aerosol aqueous phase. Atmos Chem Phys 2009;9:1907–28.

Wang G, Kawamura K, Lee S, Ho K, Cao J. Molecular, seasonal, and spatial distributions of organic aerosols from fourteen Chinese cities. Environ Sci Tech 2006a;40:4619–25.

Wang G, Kawamura K, Watanabe T, Lee S, Ho K, Cao J. High loadings and source strengths of organic aerosols in China. Geophys Res Lett 2006b;33. L22801.

Wang G, Kawamura K, Zhao X, Li Q, Niu H, Dai Z. Identification, abundance and seasonal variation of anthropogenic organic aerosols from a mega-city in China. Atmos Environ 2007;41:407–16.

Wang G, Kawamura K, Umemoto N, Xie M, Hu S, Wang Z. Water-soluble organic compounds in PM$_{2.5}$ and size-segregated aerosols over Mount Tai in North China Plain. J Geophys Res 2009;114. D19208.

Wang G, Xie M, Hu S, Gao S, Tachibana E, Kawamura K. Dicarboxylic acids, metals and isotopic compositions of C and N in atmospheric aerosols from inland China: implications for dust and coal burning emission and secondary aerosol formation. Atmos Chem Phys 2010;10:6087–96.

Wang G, Li J, Cheng C, Hu S, Xie M, Gao S, et al. Observation of atmospheric aerosols at Mt. Hua and Mt. Tai in central and east China during spring 2009 — part 1: EC, OC and inorganic ions. Atmos Chem Phys 2011;11:2611–53.

Wang G, Kawamura K, Cheng C, Li J, Cao J, Zhang R, et al. Molecular distribution and stable carbon isotopic composition of dicarboxylic acids, ketocarboxylic acids, and α-dicarbonyls in size-resolved atmospheric particles from Xi'an City, China. Environ Sci Technol 2012a;46:4783–91.

Wang G, Li J, Cheng C, Zhou B, Xie M, Hu S, et al. Observation of atmospheric aerosols at Mt. Hua and Mt. Tai in central and east China during spring 2009 — part 2: impact of dust storm on organic aerosol composition and size distribution. Atmos Chem Phys 2012b;12:4065–80.

Wang G, Zhou B, Cheng C, Cao J, Li J, Meng J, et al. Impact of Gobi desert dust on aerosol chemistry of Xi'an, inland China during spring 2009: differences in composition and size distribution between the urban ground surface and the mountain atmosphere. Atmos Chem Phys 2013;13:819–35.

Warneck P. In-cloud chemistry opens pathway to the formation of oxalic acid in the marine atmosphere. Atmos Environ 2003;37:2423–7.

Yu J, Huang X, Xu H, Hu M. When aerosol sulfate goes up, so does oxalate: implication for the formation mechanisms of oxalate. Environ Sci Tech 2005;39(1):128–33.

Zhao J, Levitt NP, Zhang R, Chen J. Heterogeneous reactions of methylglyoxal in acidic media: implications for secondary organic aerosol formation. Environ Sci Tech 2006;40:7682–7.

Zhao X, Wang X, Ding X, He Q, Zhang Z, Liu T, et al. Compositions and sources of organic acids in fine particles (PM$_{2.5}$) over the Pearl River Delta region, south China. Journal of Environ Sci 2014;26:110–21.